Energy-Efficient Precoding and Feeder-Link-Beam Matching Design for Bent-Pipe SATCOM Systems

Vu Nguyen Ha, Juan Carlos Merlano Duncan, Eva Lagunas, Jorge Querol, and Symeon Chatzinotas
Interdisciplinary Centre for Security, Reliability and Trust (SnT), University of Luxembourg, Luxembourg

***Abstract*—This paper proposes a joint optimization framework for energy-efficient linear precoding and feeder-link-beam matching design in a multi-gateway multi-beam bent-pipe satellite communication system. The proposed scheme jointly optimizes the precoding vectors at the gateway antennas and amplifying-and-matching mechanism at the satellite to maximize the system-weighted energy efficiency under the transmit power budget constraint. The technical designs are formulated into a non-convex sparsity problem consisting of a fractional-form objective function and sparsity-related constraints. To address these challenges, two iterative efficient designs are proposed by utilizing the concepts of Dinkelbach's method and the compressed-sensing approach. The simulation results demonstrate the effectiveness of the proposed scheme compared to another benchmark method.**

I. Introduction

Recently, satellite communications (SATCOM) has been considered as an important component of the next generation of wireless communication which can enable seamless global connectivity. To meet the increasing high-data-rate demand, advanced satellite communication technologies have been developed for the traditional bent-pipe payload, including multi-gateway (GW) and multi-beam (MB) transmission [1], [2]. Multiple GWs deployed in various areas can provide flexible and resilient connections between the ground segments and satellites [1]–[5] while linear precoding (LP)-enabled transmission over MBs can mitigate the interference and improve the network performance significantly [6]–[10]. Regarding both user and feeder links (FLs), this advanced SATCOM system poses significant energy-efficient (EE) challenges, including the matching and amplifying issues at the payload.

In recent years, several works have been proposed to optimize the EE of MB SATCOM systems. In [11], Chatzinotas et al. focused on investigating the EE of an MB downlink system using Minimum Mean Square Error (MMSE) LP and power optimization for the downlink channel. In [12], Qi et al. considered the design of EE multicast LP for multi-user MB SATCOMs under total power and Quality of Service (QoS) constraints. In [13], Abdu et al. proposed an EE sparse LP design for SATCOM systems, where only a few LP coefficients are used with lower transmit power consumption depending on demand. Additionally, Joroughi et al. in [14] analyze the LP scheme in a multi-GW MB satellite system. The studied design is developed by utilizing a regularized singular value block decomposition of the channel matrix to minimize both inter-cluster and intra-cluster interference. These studies demonstrate the importance of EE and LP designs in SATCOMs; however, they have not considered the impact of the FLs in their optimization frameworks.

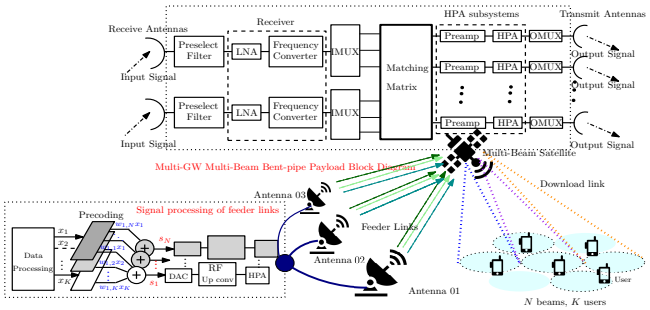

Fig. 1: Transmission diagram of a multi-GW MB bent-pipe SATCOM system.

This paper considers an end-to-end forward link of a broadband multi-GW MB bent-pipe SATCOM system serving a number of ground users. In this scheme, the ground-based LP mechanism is assumed to precoded the user signals at the GWs. The precoded are then transmitted to the satellite through MIMO-enabled transmission from multiple GW antennas (GWAs) and sub-carriers (SCs). Then, the signals over different SCs, from different GWAs are matched to the transmitting antennas of different beams before being amplified and forwarded to the users. The system poses significant challenges for EE design due to the LP tasks, matching and amplifying mechanisms, and limited transmission-power budgets. To address these challenges, we propose a joint optimization framework for EE-LP, FL-beam matching, and amplifying design. The proposed scheme optimizes the LP vectors at the GWs and sparsity variables regarding the forwarding process at the satellite to maximize the system EE (SEE) under the transmit power budget constraints. Dinkelbach's method and compressed-sensing approach are then employed to address the fractional-form objective function and sparsity-related critical issues. The work provides two solutions balancing the overall power consumption and the Quality of Service (QoS) for all users. The simulation results are also presented to highlight the superior performance of the proposed approaches in comparison to another benchmark technique.

II. System Model and Problem Formulation

A. End-to-end Multi-GW Multi-beam SATCOM Systems

Consider an end-to-end forward link of a broadband MB bent-pipe satellite system consisting of multiple GWs with L distributed antennas on the ground, a bent-pipe transparent satellite (GEO - Geostationary Equatorial Orbit, MEO - Medium Earth Orbit, or LEO - Low Earth Orbit) equipped with L receiving and N transmission elements, and K remote single-antenna users. This scheme applies LP vectors

978-1-7281-9054-9/24/$31.00 ©2024 IEEE

to the corresponding symbol sequences for users at the GW antennas. Herein, the LP can be optimized centralizedly at the central controller. These precoded signals are sent to the satellite through the multiplexing transmission from multiple GWAs and SCs. The received signals are then amplified and forwarded to the users by the satellite payload.

1) Multiplexing-enabled Feeder Links: A multiplexing transmission is assumed for the communication between the GWAs and satellite with full re-use frequency of Q/V-band [15]. Let S be the number of SCs that are channelized at each GWA in its communication with the payload; hence, the FLs from L GWAs can support at most SL streams at a specific time[1]. Here, we assume[2] $N = SL$. At these higher frequencies, links to the satellite indeed use highly directional antennas such that strong LOS connections are established. Following [15], the FL channel matrix, i.e., $\mathbf{F}$, can be modelled as $\mathbf{F} = \text{diag}\{\mathbf{F}_{(1)}, \mathbf{F}_{(2)}, ..., \mathbf{F}_{(S)}\}$. Herein, $\mathbf{F}_{(s)} \in \mathbb{C}^{L\times L}$ represents the FL channel matrix of SC s which can be expressed as

$$\mathbf{F}_{(s)} = \sqrt{G_{(s)}^{\mathsf{GWA}} G_{(s)}^{\mathsf{Sa-Rx}}}\tilde{\mathbf{F}}_{(s)}\boldsymbol{\alpha}_{(s)}, \tag{1}$$

where $G_{(s)}^{\mathsf{GWA}}, G_{(s)}^{\mathsf{Sa-Rx}}$ are the antenna gains at GWAs and satellite, $\tilde{\mathbf{F}}_{(s)} \in \mathbb{C}^{L\times L}$ models the LOS free-space propagation. Here, the (m,n)-entry of $\tilde{\mathbf{F}}_{(s)}$ is given by $[\tilde{F}^{(s)}]_{(m,n)} = \sqrt{P_{(m,n)}^{\mathsf{Loss}}}\exp\{-j(\psi_{m,n} + \phi_{m,n})\}$ where path-loss $P_{(m,n)}^{\mathsf{Loss}} = (c_0/4\pi f_{(s)}^c r_{m,n})^2$, $\psi_{m,n} = 2\pi f_{(s)}^c r_{m,n}/c_0$ and $\phi_{m,n}$ represents the miss-synchronization phase noise. $\boldsymbol{\alpha}_{(s)} \in \mathbb{C}^{L\times L}$ is a diagonal matrix of the atmospheric impairments experienced at the GWAs [15]. The l-th diagonal element of $\boldsymbol{\alpha}_{(s)}$ can be given as $\alpha_l^{(s)} = |\alpha_l|e^{-j\xi_l^{(s)}}$ where $|\alpha_l| \in (0,1]$ and $\xi_l^{(s)} \in [-\pi, \pi]$ are the amplitude fading and phase shift, respectively.

2) User Links: Let $\mathbf{H} \in \mathbb{C}^{N\times K}$ be the channel matrix of the satellite-user links. Herein, $[\mathbf{H}]_{(n,u)} = h_{n,u}$ stands for the channel coefficient from antenna n to user u which can be modeled using Rician channel model [8] as,

$$h_{n,u} = \sqrt{G_u^{\mathsf{gu}} P_u^{\mathsf{Loss}}} e^{-j(\psi_u + \phi_{n,u})}\left(\sqrt{\frac{\kappa}{\kappa+1}}p_{n,u}^{\mathsf{pa}} + \sqrt{\frac{1}{\kappa+1}}\alpha_{n,u}\right), \tag{2}$$

where G_u^{gu} is the user antenna receiving gain, path-loss $P_u^{\mathsf{Loss}} = (\lambda/4\pi d_u)^2$; $\psi_u = \frac{2\pi d_u}{\lambda}$, d_u is the distance between the satellite and user u, $p_{n,u}^{\mathsf{pa}}$ is the pattern coefficient of beam n corresponding to the user's location; $\alpha_{n,u}$ is the small NLoS fading; κ denotes Rician factor; λ is the wavelength, and $\phi^{n,u}$ stands for the phase noise.

Remark 1. *Here, $\phi_{m,n}$ and $\phi_{n,u}$, are modeled as the summation of the phase noise caused by the imperfections from the hardware components, e.g., oscillators, of the GWAs, satellite payload and the users' receivers.*

3) Ground-based LP Design: Due to N transmission elements, one assumes the satellite can generate at most N satellite beams for user-link transmission. Let $\mathbf{w}_u = [w_{1,u}, w_{2,u}, ..., w_{N,u}]^T \in \mathbb{C}^{N\times 1}$ be the LP vector designed for symbol sequence of user u, named $x_u \in \mathbb{C}$ and $\mathbb{E}_{x_u}\{|x_u|\} = 1$. Considering the signal processing design, the GWs first apply all LP vector $\mathbf{w}_u$'s to the symbol sequences of all users. The precoded signals can be written as $\mathbf{s} = \sum_{u\in\mathcal{U}}\mathbf{w}_u x_u \in \mathbb{C}^{N\times 1}$, where $\mathcal{U}$ stands for the set of users. Then, $\mathbf{s}$ is sent to the satellite over N FL SCs from L GWAs. The received signal at the satellite can be expressed as

$$\mathbf{r} = \mathbf{F}^H\mathbf{s} + \mathbf{n}^{\text{fd}} = \mathbf{F}^H\sum_{u\in\mathcal{U}}\mathbf{w}_u x_u + \mathbf{n}^{\text{fd}}, \tag{3}$$

where $\mathbf{n}^{\text{fd}} \in \mathbb{C}^{N\times 1}$ is an AWGN vector at the satellite.

4) Payload Matching and Amplifying Process: At the satellite, N signal streams corresponding to N FL SCs, i.e $\mathbf{r}$, are amplified and then matched to N beams for propagation to users over the user links. To ease the notation, we name FL t as the FL SC that carries the precoded symbol stream corresponding to t-th element of $\mathbf{s}$. Let $\mathbf{B} \in \mathbb{R}_+^{N\times N}$ be the N-stream-to-N-beam amplifying and matching matrix. Denote $[\mathbf{B}]_{n,t} = b_{n,t}$ as an element locating on the t-th row and n-th column of $\mathbf{B}$, we have $b_{n,t} > 0$ if $[\mathbf{r}]_t$ is transmitted over beam n, and $b_{n,t} = 0$ otherwise. Due to the matching policy, $\mathbf{B}$ must be designed by regarding the following constraints,

$$(C1): \sum_{\forall t}\|b_{n,t}\|_0 \le 1, \forall n, \text{ and } (C2): \sum_{\forall n}\|b_{n,t}\|_0 \le 1, \forall t, \tag{4}$$

where $\|x\|_0$ stands for the norm-0 of x. Multiplying $\mathbf{B}$ to $\mathbf{r}$ at the payload and then forwarding the amplified signal to users, one yields the received signal at all users as

$$\mathbf{z} = \mathbf{H}^H\mathbf{B}\mathbf{r} + \mathbf{n}^{\text{dl}} = \mathbf{H}^H\mathbf{B}(\mathbf{F}^H\mathbf{s} + \mathbf{n}^{\text{fd}}) + \mathbf{n}^{\text{dl}}, \tag{5}$$

where $\mathbf{n}^{\text{dl}} \in \mathbb{C}^{K\times 1}$ is an AWGN vector. Note that the u-th column of $\mathbf{H}$, i.e., $\mathbf{h}_u = [h_{1,u}, h_{2,u}, ..., h_{N,u}]^T$, represents the channel vector from satellite to user u. Then, the received signal given in (5) yields the SINR at user u as

$$\Gamma_u(\mathbf{W},\mathbf{B}) = \frac{\left|\mathbf{h}_u^H\mathbf{B}\mathbf{F}^H\mathbf{w}_u\right|^2}{\sum_{i\neq u}\left|\mathbf{h}_u^H\mathbf{B}\mathbf{F}^H\mathbf{w}_i\right|^2 + \mathbf{h}_u^H\mathbf{B}\Sigma\mathbf{B}^T\mathbf{h}_u + \sigma_u^{\text{dl}2}}, \tag{6}$$

where $\mathbf{W} = [\mathbf{w}_1, \mathbf{w}_2, ...\mathbf{w}_K] \in \mathbb{C}^{N\times K}$, $\sigma_u^{\text{dl}2}$ and $\Sigma = \text{diag}[\sigma_1^{\text{fd}2}, \sigma_2^{\text{fd}2}, ..., \sigma_N^{\text{fd}2}]$ represent the noise power at user u and the noise covariance matrix at satellite, respectively. Learning from (6), one can estimate the total achievable rate by the Shanon upper bound, as follows

$$R_{\text{tot}}(\mathbf{W},\mathbf{B}) = R_s\sum_{\forall u}\log_2\left(1 + \Gamma_u(\mathbf{W},\mathbf{B})\right). \tag{7}$$

where R_s is the baud-rate of the user links.

Remark 2. *Note that, $\mathbf{B} = \text{diag}(\boldsymbol{\xi})\mathbf{A}$ where $\mathbf{A}$ is a permutation matrix with $[\mathbf{A}]_{n,t} = a_{n,t} = \|b_{n,t}\|_0$ while ξ_n is the amplify factor corresponding to beam n and $\boldsymbol{\xi} = [\xi_1, ..., \xi_N]^T$.*

B. Power Consumption Model

1) Gateway Power Consumption: Besides the transmission power, the consumed component corresponding to the RF signal processing mainly depends on the number of FL subcarriers and activated beams. Once, an FL SC is utilized, the

[1]For instance, 4GHz bandwidth over the Q/V band is channelized into 16 250 MHz SCs. One SC carries one data stream without OFDM employed.

[2]It required to note if $N > SL$, then the TDMA can be employed to transmit N streams from GWAs to the satellite. And, if $N < SL$, one can select N links to form a $N \times N$ FL channel matrix.

corresponding precoded base-band signal goes through the DAC before being up-converted to the RF band, amplified by the HPA, and propagated to the satellite over that SC. The transmission power relating to FL t can be described as $P_t^{\mathsf{GWA}} = \sum_{\forall u} \mathbf{w}_u^H \mathbf{E}_t \mathbf{w}_u$, where $\mathbf{E}_t$ is a diagonal matrix in $\mathbb{R}^{N\times N}$ with zero elements and one at the t-th position. Note that FL t is utilized if and only if $P_t^{\mathsf{GWA}} > 0$. Then, the number of utilized FLs can be described as $T_{\text{fd}} = \sum_{\forall t} \|P_t^{\mathsf{GWA}}\|_0$. Moreover, the power consumption of HPA for FL transmission can be modeled as $P^{\text{PA}}_{\mathsf{GWA},t} = (1/\rho_{\mathsf{GWA}})(P_t^{\mathsf{GWA}} - P_{\text{bb}})$, [16]in which ρ_{GWA} stands for the HPA efficiency and P_{bb} is the base-band signal power. Then, the RF signal processing and propagation power consumption of all GWAs is

$$\begin{aligned} P_{\mathsf{GWA}}(\mathbf{W}) &= P^{\text{hw}}_{\mathsf{GWA}} T_{\text{fd}} + \sum_{\forall t} \left(P^{\text{PA}}_{\mathsf{GWA},t} + P_t^{\mathsf{GWA}} \right) \\ &= P^{\text{hw}}_{\mathsf{GWA}} \sum_{\forall t} \|P_t^{\mathsf{GWA}}\|_0 + \tfrac{\rho_{\mathsf{GWA}}+1}{\rho_{\mathsf{GWA}}} \sum_{u\in\mathcal{U}} \mathbf{w}_u^H \mathbf{w}_u, \end{aligned} \tag{8}$$

where $P^{\text{hw}}_{\mathsf{GWA}}$ is the total power of DAC, RF up-converter components, and $-P_{\text{bb}}/\rho_{\mathsf{GWA}}$. Here, we assume that $P^{\text{hw}}_{\mathsf{GWA}} > 0$.

2) Satellite Power Consumption: According to the bent-pipe transponder illustrated in Fig. 1, the satellite power consumption can be estimated as

$$\begin{aligned} &P_{\text{Sa}}(\mathbf{W},\mathbf{B}) = P^{\text{hw}}_{\text{Sat}} T_{\text{fd}} + P^{\text{PA}}_{\text{Sa}} + P^{\text{dl}}_{\text{Tx}} \\ &= P^{\text{hw}}_{\text{Sat}} \sum_{\forall (t,n)} \|P_t^{\mathsf{GWA}}\|_0 + \tfrac{\rho_{\text{Sa}}+1}{\rho_{\text{Sa}}} \Big(\sum_{u\in\mathcal{U}} \mathbf{w}_u^H \mathbf{F}\mathbf{B}^T \mathbf{B}\mathbf{F}^H \mathbf{w}_u + \text{Tr}(\mathbf{B}\Sigma\mathbf{B}^T) \Big) \\ &\qquad - (1/\rho_{\text{Sa}}) \Big(\sum_{u\in\mathcal{U}} \mathbf{w}_u^H \mathbf{F}\mathbf{F}^H \mathbf{w}_u + \text{Tr}(\Sigma) \Big), \end{aligned} \tag{9}$$

where $P^{\text{hw}}_{\text{Sat}}$ is for the power of satellite hardware components, $P^{\text{dl}}_{\text{Tx}}$ is the transmission power and $P^{\text{PA}}_{\text{Sa}} = (1/\rho_{\text{Sa}})(|\mathbf{B}\mathbf{r}|^2 - |\mathbf{r}|^2)$ implies the HPA power in which ρ_{Sa} is the power amplifier efficiency at the satellite [16].

3) Total Weighted Power Consumption: From the engineering point of view, we aim to utilize various weights for power consumption from GWAs and satellite due to the different energy budgets of these system components. In particular, a higher weight should be marked for satellite due to its limited power-supply sources. Let δ^{GWA} and δ^{Sa} be the impacting weights corresponding to the power consumption of GWAs and satellite, respectively. Then, the total weighted power consumption can be expressed as

$$P_{\text{tot}}(\mathbf{W},\mathbf{B}) = \delta^{\mathsf{GWA}} P_{\mathsf{GWA}}(\mathbf{W}) + \delta^{\mathsf{Sa}} P_{\text{Sa}}(\mathbf{W},\mathbf{B}). \tag{10}$$

C. Problem Formulation

We are now ready to define the ratio of the sum rate to the total weighted power consumption, so-called system weighted energy efficiency (SWEE) in bits/W, as

$$\eta(\mathbf{W},\mathbf{B}) = R_{\text{tot}}(\mathbf{W},\mathbf{B}) / P_{\text{tot}}(\mathbf{W},\mathbf{B}). \tag{11}$$

In this paper, we are interested in jointly optimizing the LP vectors at the GWs, and the matching and amplifying gains at the satellite to maximize the SWEE under the constraint on the transmit power budget at each antenna. This SWEE maximization (SWEEM) problem can be stated as

$$\max_{\mathbf{W},\mathbf{B}} \ \eta(\mathbf{W},\mathbf{B}) = R_{\text{tot}}(\mathbf{W},\mathbf{B}) / P_{\text{tot}}(\mathbf{W},\mathbf{B}) \tag{12a}$$

Algorithm 1: Overview of the Proposed Algorithm

1: Initialize $\eta^{(0)} = 0$, set $\ell = 0$, and choose a tolerate τ^{out}.
2: **repeat**
3: Solve (13) with $\eta^{(\ell)}$ to achieve $(\mathbf{W}^{(\ell)}, \mathbf{B}^{(\ell)})$.
4: Update $\eta^{(\ell+1)} = \frac{R_{\text{tot}}(\mathbf{W}^{(\ell)},\mathbf{B}^{(\ell)})}{P_{\text{tot}}(\mathbf{W}^{(\ell)},\mathbf{B}^{(\ell)})}$.
5: Set $\ell := \ell + 1$.
6: **until** $|\eta^{(\ell)} - \eta^{(\ell-1)}| \le \tau^{\text{out}}$.
7: Return $(\mathbf{W}^{(\ell-1)}, \mathbf{B}^{(\ell-1)})$.

$$\text{s. t.} \quad \text{constraints } (C1), (C2),$$

$$(C3): \sum_{\forall u} \mathbf{w}_u^H \mathbf{E}_t \mathbf{w}_u \le \bar{P}_t^{\mathsf{GWA}}, \forall t, \tag{12b}$$

$$(C4): \sum_{\forall t} b_{n,t}^2 \Big(\sum_{u\in\mathcal{U}} \mathbf{w}_u^H \mathbf{F}\mathbf{E}_t\mathbf{F}^H \mathbf{w}_u + {\sigma_t^{\text{fd}}}^2 \Big) \le \bar{P}_n^{\text{Sa}}, \forall n, \tag{12c}$$

where $(C3)$ and $(C4)$ are considered based on the transmission power budget of each FL at the GWs and every antenna of the satellite, respectively. As can be seen, problem (12) is an NP-hard mixed integer programming. To deal with this complicated problem, we aim to employ Dinkelbach's method [17] and compressed-sensing approach to cope with the fractional-form critical issue and mixed-integer challenge.

III. Proposed Solution Approaches

A. The Foundation of Dinkelbach Method

This method is summarized in the following theorem [17].

Theorem 1. *Let η^* be the optimal objective value of problem $(\mathcal{P}_I) : \max_{\mathbf{x}} R(\mathbf{x})/P(\mathbf{x})$ s. t. $\mathbf{x} \in \mathcal{S}$, where $P(\mathbf{x}) > 0$ $\forall \mathbf{x} \in \mathcal{S}$. Consider the subtracting-form problem $\left(\mathcal{P}_{II}^{(\eta)}\right) : \max_{\mathbf{x}} R(\mathbf{x}) - \eta P(\mathbf{x})$ s. t. $\mathbf{x} \in \mathcal{S}$. Denote $\chi(\eta)$ as the optimal objective value of $\left(\mathcal{P}_{II}^{(\eta)}\right)$ for given η. Then, $\chi(\eta)$ is a function of η which has the following characteristics:*

i) *$\chi(\eta)$ is a strictly monotonic decreasing function.*
ii) *$\chi(\eta) > 0$ if and only if $\eta < \eta^*$, vice versa.*
iii) *$(\mathcal{P}_I)$ and $\left(\mathcal{P}_{II}^{(\eta^*)}\right)$ have the same set of optimal solutions.*

Proof: The proof can be found in [16], [17]. ■

Theorem 1 prompts us to develop an iterative approach to obtain the optimal solution of problem (12) which is summarized in Algorithm 1. In particular, we first state the parameterized problem for a given value of η as follows.

$$\max_{\mathbf{W},\mathbf{B}} R_{\text{tot}}(\mathbf{W},\mathbf{B}) - \eta P_{\text{tot}}(\mathbf{W},\mathbf{B}) \text{ s.t. } (C1) - (C4). \tag{13}$$

Then, the algorithm tends to iteratively solve problem (13) for a certain value of η, and adjust η until an optimal $\eta^\star \ge 0$ satisfying $R_{\text{tot}}(\mathbf{W},\mathbf{B}) - \eta^\star P_{\text{tot}}(\mathbf{W},\mathbf{B}) = 0$ is found. In what follows, we will propose two novel approaches dealing with problem (13) in **Step 3** of Algorithm 1 efficiently.

B. Joint Linear Precoding and FL-Beam Matching Design

The challenges of solving problem (13) come from the non-convex objective function and the sparsity terms. To address these, the MMSE-based transformation [8] and the CS method can be exploited as follows.

1) MMSE-based Transformation: We first relate the logarithm-formed rate to a weighted sum-mean square error (MSE) minimization problem in the following theorem.

Theorem 2. *Problem* (13) *is equivalent to the following,*

$$\min_{\mathbf{W},\mathbf{B}} \eta P_{\text{tot}}(\mathbf{W},\mathbf{B}) + R_s \sum_{\forall u}(\omega_u e_u - \log \omega_u) \;\; s.t. \;\; (C1)-(C4), \quad (14)$$

where $e_u = \mathbb{E}[|x_u - \delta_u z_u|^2]$, ω_u *and* δ_u *represent the MSE weight and the receive coefficient for user u, respectively.*

Proof: The proof is similar to that given in [8]. ∎

It is noted that problem (14) is not *jointly* convex, it is convex over each set of variables $\mathbf{W}$, $b_{n,t}$'s, δ_u's, and ω_u's. Thus, one can solve problem (14) by alternately optimizing over one set of variables while keeping the others fixed.

2) Update MSE Weights and Receive Coefficients: Handling some minor manipulation on $e_u = \mathbb{E}[|x_u - \delta_u z_u|^2]$ and taking the corresponding derivative, δ_u's can be optimized in order to minimize e_u for given $(\mathbf{W},\mathbf{B})$ as

$$\delta_u^\star = \mathbf{\Theta}_u^{-1} \mathbf{w}_u^H \mathbf{F}\mathbf{B}^T \mathbf{h}_u, \quad (15)$$

where $\mathbf{\Theta}_u = \sum_{\forall i} \left|\mathbf{h}_u^H \mathbf{B}\mathbf{F}^H \mathbf{w}_i\right|^2 + \mathbf{h}_u^H \mathbf{B}\Sigma\mathbf{B}^T \mathbf{h}_u + {\sigma_u^{\text{dl}}}^2$. Again, by taking the derivative of the objective function in (14) with respective to ω_u, the optimum value $\omega_u^\star$ can be expressed as

$$\omega_u^\star = e_u^{-1} = \left(1 - \mathbf{\Theta}_u^{-1} \left|\mathbf{h}_u^H \mathbf{B}\mathbf{F}^H \mathbf{w}_u\right|^2\right)^{-1}. \quad (16)$$

3) Linear Precoding and Amplifying Matrix Design: We are now ready to develop an efficient mechanism to due with (14) for given δ_u's and ω_u's. As can be observed, the challenges of solving $\mathbf{W}$ and $\mathbf{B}$ come from the norm-ℓ_0 forms of both of these variables in the power consumption formulas and constraints $(C1)-(C2)$. To simply such difficulty corresponding $\mathbf{W}$, we transform the term $\|P_t^{\mathsf{GWA}}\|_0$ into the sparsity form of $\mathbf{B}$ by regarding the following lemma.

Lemma 1. *Regarding the optimal solutions of problems* (12) *(also* (13) *and* (14)*), the following equality can be hold,*

$$\|P_t^{\mathsf{GWA}}\|_0 = \|\sum_{\forall n} b_{n,t}\|_0 = \sum_{\forall n} \|b_{n,t}\|_0, \quad \forall t. \quad (17)$$

Proof: As can be seen, if $P_t^{\mathsf{GWA}} = 0$ which implies that FL t is not activated; then, $b_{n,t} = 0$ for all n can be an efficient solution. Inversely, $\sum_{\forall n} b_{n,t} = 0$ shows that no beam will forward the signal from FL t to users. In such scenarios, to achieve better solutions, P_t^{GWA} must be zeros. ∎

Thanks to Lemma 1 and regrading that $e_u = [1 + |\delta_u|^2 \mathbf{\Theta}_u - 2\Re\left(\delta_u' \mathbf{w}_u^H \mathbf{F}\mathbf{B}^T \mathbf{h}_u\right)]$, one can rewrite problem (13) for given δ_u's and ω_u's as

$$\begin{aligned}\min_{\mathbf{W},\mathbf{B}} \; & \text{Tr}((\nu_3\mathbf{I} + \Lambda)\mathbf{B}\Sigma\mathbf{B}^T) - 2\sum_{u\in\mathcal{U}} \Re(\omega_u \delta_u' \mathbf{w}_u^H \mathbf{F}\mathbf{B}^T \mathbf{h}_u) \\ & + \sum_{\forall u} \mathbf{w}_u^H [\nu_1\mathbf{I} - \nu_2 \mathbf{F}\mathbf{F}^H + \mathbf{F}\mathbf{B}^T(\nu_3\mathbf{I} + \Lambda)\mathbf{B}\mathbf{F}^H]\mathbf{w}_u + \nu^{\text{hw}} \sum_{\forall (t,n)} \|b_{n,t}\|_0, \\ \text{s. t.} \;\; & \text{constraints } (C1) - (C4), \end{aligned} \quad (18)$$

where $\Re(.)$ stands for the real part, $\nu^{\text{hw}} = \frac{\eta}{R_s}(\delta^{\mathsf{GWA}} P_{\mathsf{GWA}}^{\text{hw}} + \delta^{\mathsf{Sa}} P_{\text{Sa}}^{\text{hw}})$, $\nu_1 = \frac{\eta\delta^{\mathsf{GWA}}}{R_s}\frac{\rho_{\mathsf{GWA}}+1}{\rho_{\mathsf{GWA}}}$, $\nu_2 = \frac{\eta\delta^{\mathsf{Sa}}}{\rho_{\text{Sa}} R_s}$, $\nu_3 = \frac{\eta\delta^{\mathsf{Sa}}}{R_s}\frac{\rho_{\text{Sa}}+1}{\rho_{\text{Sa}}}$, and $\Lambda = \sum_{\forall i} \omega_i |\delta_i|^2 \mathbf{h}_i \mathbf{h}_i^H$.

a) Linear Precoding Design: For given $\mathbf{B}$, the corresponding LP vectors can be determined by solving the following Quadratically Constrained Quadratic Program (QCQP),

$$\min_{\mathbf{W}} \sum_{\forall u} \mathbf{w}_u^H \mathbf{\Pi} \mathbf{w}_u - 2\Re(\mathbf{w}_u^H \mathbf{k}_u) \text{ s.t. } (C3) \text{ and } (C4), \quad (19)$$

where $\mathbf{\Pi} = \nu_1\mathbf{I} - \nu_2\mathbf{F}\mathbf{F}^H + \mathbf{F}\mathbf{B}^T(\nu_3\mathbf{I} + \Lambda)\mathbf{B}\mathbf{F}^H$ and $\mathbf{k}_u = \omega_u \delta_u' \mathbf{F}\mathbf{B}^T \mathbf{h}_u$. This QCQP problem can be solved effectively by employing some standard convex optimization solvers.

b) Sparsity Amplifying Matrix Design: To deal with the norm-ℓ_0 challenge of solving $\mathbf{B}$, one can employ the re-weighted norm-ℓ_1 approximation methods which have been proposed to enhance the data acquisition in compressed sensing. In particular, the sparsity term $\|b_{n,t}\|_0$ can be approximated to $\beta_{n,t} b_{n,t}$ where $\beta_{n,t}$ is a re-weighted factor. In the CS approach, a such factor can be chosen as [18]–[20]

$$\beta_{n,t} = \sqrt{1/(b_{n,t}^2 + \epsilon)}, \quad (20)$$

where $\epsilon \ll 1$. Note that $\beta_{n,t}$ can be updated so that the closed-to-zero elements in the previous iteration will suffer a huge penalty. Denote $\mathbf{b}_t \in \mathbb{C}^{N\times 1}$ as the vector generated from the t-th column of $\mathbf{B}$. Regarding that $\|b_{n,t}\|_0 = \|b_{n,t}^2\|_0$, we can rewrite the sparsity terms in (18) as

$$\sum_{\forall n} \|b_{n,t}\|_0 = \mathbf{b}_t^T \mathbf{D}_t \mathbf{b}_t \text{ and } \sum_{\forall t} \|b_{n,t}\|_0 = \sum_{\forall t} \mathbf{b}_t^T \mathbf{E}_{n,t} \mathbf{b}_t, \quad (21)$$

where $\mathbf{D}_t = \mathsf{Diag}(\beta_{1,t}^2, ..., \beta_{N,t}^2)$ and $\mathbf{E}_{n,t}$ is a zero matrix except that its n-th diagonal element is $\beta_{n,t}^2$. Then, we introduce vector $\mathbf{b} \in \mathbb{C}^{N^2\times 1}$ which is $\mathbf{b} = [\mathbf{b}_1; ...; \mathbf{b}_N]$. By properly choosing and updating $\beta_{n,t}$'s, problem (18) for given $\mathbf{W}$ can be relaxed to the following QCQP problem,

$$\min_{\mathbf{B}} \mathbf{b}^T(\mathbf{\Psi} + \nu^{\text{hw}}\mathbf{D} + \nu_3\tilde{\mathbf{\Sigma}})\mathbf{b} - \tilde{\mathbf{f}}^T\mathbf{b} \text{ s.t. } (\tilde{C}1): \mathbf{b}^T\tilde{\mathbf{D}}_t\mathbf{b} \le 1, \forall t, \quad (22a)$$

$$(\tilde{C}2): \mathbf{b}^T\mathbf{E}_n\mathbf{b} \le 1, \forall n, \text{ and } (\tilde{C}4): \mathbf{b}^T\mathbf{\Gamma}_n\mathbf{b} \le \bar{P}_n^{\text{Sa}}, \forall n, \quad (22b)$$

where $\mathbf{D} = \mathsf{BlkDiag}(\mathbf{D}_1; ..., \mathbf{D}_N)$; $\tilde{\mathbf{\Sigma}} = \mathsf{BlkDiag}(\sigma_1^{\text{fd}^2}\mathbf{I}, ..., \sigma_N^{\text{fd}^2}\mathbf{I})$; $\mathbf{\Psi} \in \mathbb{C}^{N^2\times N^2}$ and its (n,t)-th $N\times N$ block matrix is defined as $[\mathbf{\Psi}]_{(n,t)} = (\nu_3\mathbf{I} + \sum_{\forall u}\omega_u|\delta_u|^2\mathbf{h}_u\mathbf{h}_u^H)(\sum_{\forall i}\mathbf{w}_i^H\mathbf{f}_n\mathbf{f}_t^H\mathbf{w}_i)$; $\tilde{\mathbf{f}} \in \mathbb{R}^{N^2\times 1}$ and its t-th $N\times 1$ block vector is defined as $[\tilde{\mathbf{f}}]_t = 2\Re(\sum_{\forall u}\omega_u\delta_u'\mathbf{h}_u\mathbf{w}_u^H\mathbf{f}_t)$; $\tilde{\mathbf{D}}_t \in \mathbb{C}^{N^2\times N^2}$ contains all zeros except that its (t,t)-th $N\times N$ block matrix is $\mathbf{D}_t$; $\mathbf{E}_n = \mathsf{BlkDiag}(\mathbf{E}_{n,1}; ...; \mathbf{E}_{n,N})$; and $\mathbf{\Gamma}_n = \mathsf{BlkDiag}(\gamma_1\mathbf{E}_{n,1}; ...; \gamma_N\mathbf{E}_{n,N})$ in which $\gamma_t = \sum_{\forall u}\mathbf{w}_u^H\mathbf{f}_t\mathbf{f}_t^H\mathbf{w}_u + \sigma_t^{\text{fd}^2}$. Herein, $\mathbf{f}_t$ represents the vector generated from t-th column of $\mathbf{F}$. This QCQP problem can also be solved by employing some *off-the-shelf* convex optimization solvers.

4) Joint LP and FL-Beam Matching Algorithm: By iteratively updating $\beta_{n,t}$'s and alternatively determining ω_u's, δ_u's, $\mathbf{W}$, $\mathbf{B}$ as described above, the solution of (13) can be obtained. The solution approach is summarized in Algorithm 2. Then, the system energy efficiency (SEE) results can be obtained by integrating Algorithms 1 and 2, which is also named as *joint LP and FL-beam matching* (JPFBM) mechanism.

Remark 3. *Giving the convergence proof of this algorithm is challenging due to the lack of space. However, convergence can be guarantee by Dinkelbach Method, the well-known*

Algorithm 2: ITERATIVE JOINT LP AND FL-BEAM MATCHING DESIGN

1: Initialize: Select suitable $\mathbf{W}^{[0]}$, and small ϵ and set $\mathbf{B}^{[0]} = \mathbb{1}_{N\times N}$. Set $k = 0$.
2: **repeat**
3: Update $k := k + 1$.
4: Calculate $\{\delta_u^{[k]}, \omega_u^{[k]}\}$'s as in (15), (16) based on $\mathbf{W}^{[k-1]}$, $\mathbf{B}^{[k-1]}$.
5: Optimize $\mathbf{W}^{[k]}$ by solving problem (19).
6: Update $\beta_{n,t}$'s as in (20).
7: Optimize $\mathbf{B}$ by solving problem (22).
8: **until** Convergence of the objective function in (14).

Algorithm 3: JOINT LP WITH AMPLIFY-AND-FORWARD DESIGN

1: Initialize:
- Define a matching matrix $\mathbf{A}$ satisfying $(C1)$ and $(C2)$.
- Select suitable $\mathbf{W}^{[0]}$, and small ϵ, and set $\boldsymbol{\xi}^{[0]} = \mathbb{1}_{N\times 1}$. Set $k = 0$.

2: **repeat**
3: Update $k := k + 1$.
4: Define $\{\delta_u^{[k]}, \omega_u^{[k]}\}$'s as in (15), (16) based on $\mathbf{W}^{[k-1]}$, $\mathbf{A}$, $\boldsymbol{\xi}^{[k-1]}$.
5: Optimize $\mathbf{W}^{[k]}$ by solving problem (19).
6: Update α_t's as $\alpha_t = \sqrt{1/(\xi_t^2 + \epsilon)}$, Optimize $\boldsymbol{\xi}$ by solving problem (23).
7: **until** Convergence of the objective function in (14).

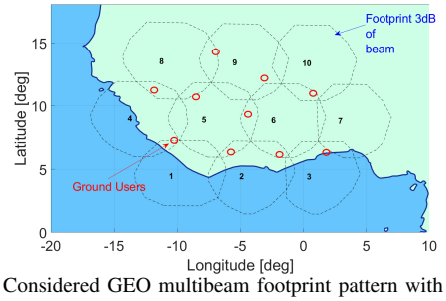

Fig. 2: Considered GEO multibeam footprint pattern with $N = 10$.

compressed-sensing approach, as well as the goal of updating $\{\delta_u, \omega_u\}$*'s,* $\mathbf{W}$*, and* $\mathbf{B}$ *which aims to keep the objective of problem* (14) *monotonically decreasing.*

C. Low-Complex Solution Approach for given Matching

Thanks to Remark 2, we aim to optimize the LP and amplifying designs for a given FL-beam matching solution. Note that the corresponding amplifier gain should be set to zero when FL t is inactivated, which yields $\|P_t^{\mathsf{GWA}}\|_0 = \|\xi_t\|_0$. Re-employing the compressed-sensing approach for treating variables $\boldsymbol{\xi}$, we introduce the re-weight factor α_t as $\alpha_t = \sqrt{1/(\xi_t^2 + \epsilon)}$. Then, for given $\mathbf{A}$, problem (22) can be stated as

$$\min_{\boldsymbol{\xi}} \boldsymbol{\xi}^T (\boldsymbol{\Phi} + \nu^{\mathsf{hw}}\mathbf{L})\boldsymbol{\xi} - \mathbf{c}^T \boldsymbol{\xi} \text{ s.t. } \xi_n^2 \sum_{\forall t} a_{n,t}\gamma_t \le \bar{P}_n^{\mathrm{Sa}}, \forall n, \quad (23)$$

where $\boldsymbol{\Phi} \in \mathbb{C}^{N\times N}$ and its (n,t)-th elements is defined as $\boldsymbol{\Phi}_{(n,t)} = \mathbf{a}_n^T [\boldsymbol{\Psi}]_{(n,t)} \mathbf{a}_t$; $\mathbf{L} = \mathsf{Diag}(\alpha_1^2, ..., \alpha_N^2)$; $\mathbf{c} \in \mathbb{R}^{N\times 1}$ and its t-th element is defined as $c_t = \mathbf{a}_t^T [\tilde{\mathbf{f}}]_t$. This problem is also a QCQP where $\boldsymbol{\xi} \in \mathbb{R}^{N\times 1}$; hence, $\boldsymbol{\xi}$ can be defined optimally by employing some *off-the-shelf* optimization tools. Then, the proposed continuous-rate AF precoding design framework is summarized in Algorithm 3. Then, the SEE results are obtained by integrating Algorithms 1 and 3, which is also called *joint LP with amplify-and-forward* (JPAF) approach.

TABLE I: Simulation Parameters

GW Hardware-Power	10 W
[49.075, 49.325, 49.575, 49.825, 50.075] (GHz)	FL subcarrier ($S = 5$)
GW antenna diameter [21]	6.8 m
Satellite Orbit	13°E (GEO)
GEO Rx antenna diameter [15]	1.4 m
Separation between 2 GEO Rx-antennas [15]	3 m
Miscellaneous losses [15]	1 dB
Beam Hardware-Power	5 W
Beam Radiation Pattern	Provided by ESA
Downlink Carrier Frequency	19.5 GHz
User Link Bandwidth, R_s	250 MHz
Noise Power at Satellite and Users	−121.3 and −118.6 dB

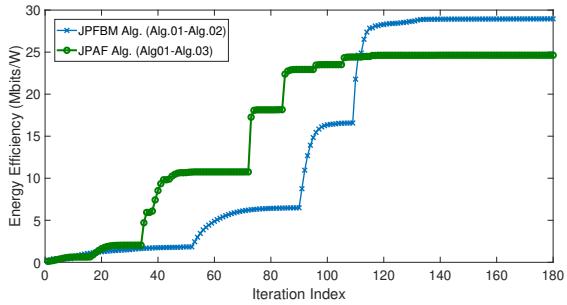

Fig. 3: System EE obtained by JPFBM and JPAF algorithms.

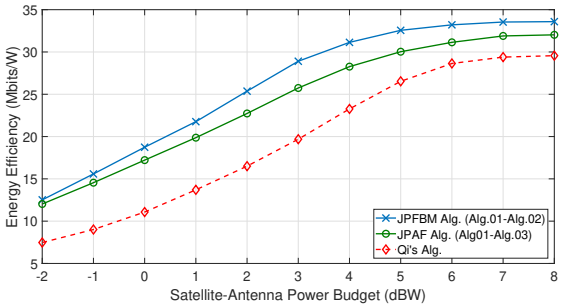

Fig. 4: The SEE versus the transmit power budget of each satellite antenna.

IV. SIMULATION RESULTS

We consider a GEO satellite system with 10 spot beams serving 10 users, i.e., $N = 10$ and $K = 10$, as shown in Fig. 2. Two GWAs located in Redu (Belgium), and Betzdorf (Luxembourg) with (lat, lon) coordinates of $(50.002461, 5.148105)$ and $(49.692915, 6.327135)$ are assumed. Other setting parameters are summarized in Table I. In addition, the efficiency factors of all antennas and HPAs are set at 60% and $\mathbf{A} = \mathbf{I}_{N\times N}$.

First, we investigate the convergence of our proposed algorithms by presenting the SEE results obtained by the JPFBM and JPAF frameworks over iterations in Fig. 3. Here, $\bar{P}_t^{\mathsf{GWA}} = 15$ dBW and $\bar{P}_n^{\mathrm{Sat}} = 5$ dBW, and we consider the total power consumption of the system by setting $\delta^{\mathsf{GWA}} = \delta^{\mathrm{Sa}} = 1$. As observed, the SEEs for both approaches increase and plateau after around 100 iterations, confirming the convergence of our proposed frameworks. Upon convergence, the JPFBM framework yields a higher SEE compared to the JPAF one.

Next, Fig. 4 depicts the SEE achieved by our proposed frameworks, as well as of Qi's method [12], with respect to varying values of $\bar{P}_n^{\mathrm{Sa}}$, the transmission power budget for each satellite antenna. Note that Qi's work only focuses on satellite power consumption in their SEE formula. To ensure

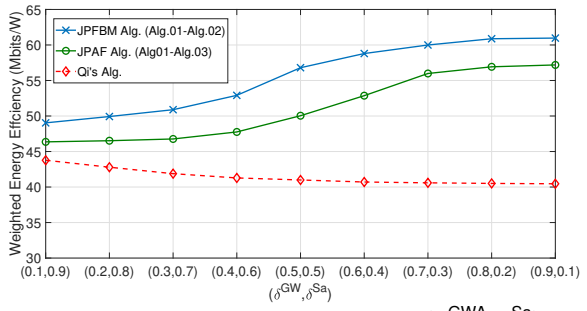

Fig. 5: The SWEE versus various values of $(\delta^{\mathsf{GWA}}, \delta^{\mathsf{Sa}})$.

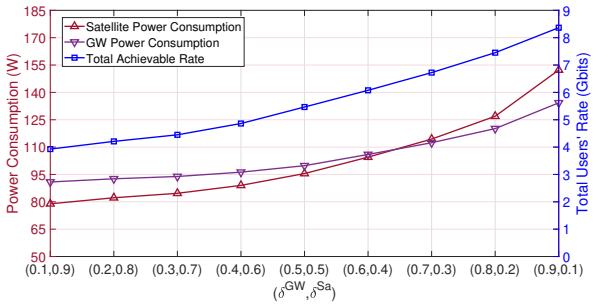

Fig. 6: The JPFBM sum rate and power consumption vs. $(\delta^{\mathsf{GWA}}, \delta^{\mathsf{Sa}})$.

a fair comparison, we set $\mathbf{B} = \left(\mathbf{F}^H\mathbf{F}\right)^{-1/2}$ and carry out simple manipulations to estimate the GW power consumption in this approach. Here, $\bar{P}_t^{\mathsf{GWA}} = 15$ dBW. As expected, all three methods can achieve higher SEEs as $\bar{P}_n^{\mathsf{Sa}}$ increases. At the high regime of $\bar{P}_n^{\mathsf{Sa}}$, SEEs of these three tend to saturate due to the limitation in FL transmission. The figure also reveals that our proposed JPFBM and JPAF mechanisms surpass Qi's algorithm while JPFBM performs better than JPAF.

Finally, Figs. 5 and 6 illustrate the variations in SWEE, achievable rate, and power consumption of JPFBM mechanism across different values of $(\delta^{\mathsf{GWA}}, \delta^{\mathsf{Sa}})$. In this simulation, we set $\bar{P}_t^{\mathsf{GWA}} = 15$ dBW, $\bar{P}_n^{\mathsf{Sat}} = 5$ dBW, vary $(\delta^{\mathsf{GWA}}, \delta^{\mathsf{Sa}})$ such that $\delta^{\mathsf{GWA}} + \delta^{\mathsf{Sa}} = 1$. In Fig. 5, the SWEE of our proposed JPFBM and JPAF mechanisms increases while that of Qi's method decreases as δ^{GWA} increases. Once again, our proposed approaches outperform Qi's method across all power-weight configurations, and the JPFBM mechanism provides superior. These results clearly emphasize the benefits of employing the jointly designed LP and FL-beam matching mechanism in the multi-GW, multi-beam SATCOM systems. In Fig. 6, one depicts that all rate and power consumption enlarge as δ^{GWA} increases. These outcomes shown in Figs. 5 and 6 suggest that the user links have a more significant impact on the network performance compared to the FLs.

V. Conclusion

This paper presented a joint optimization framework for energy-efficient precoding and FL-beam matching design in multi-GW, multi-beam bent-pipe SATCOM systems which aims to maximize the SWEE. The technical designs were formulated as a non-convex sparsity problem. Two iterative efficient designs have been proposed to tackle these challenges by employing Dinkelbach and CS approach. The simulation results showcased the effectiveness and superiority of the proposed JPFBM and JPAF frameworks over another benchmark.

Acknowledgment

This research was funded in whole by the Luxembourg National Research Fund (FNR), with two granted projects corresponding to three grant references C23/IS/18073708/SENTRY (SENTRY project), C21/IS/16352790/ARMMONY (ARMMONY), and C19/IS/13696663/FLEXSAT (FlexSAT).

References

[1] G. Fontanesi and et al., "Artificial intelligence for satellite communication and non-terrestrial networks: A survey," in *arXiv.2304.13008*, 2023.
[2] V. N. Ha, E. Lagunas, T. S. Abdu, H. Chaker, S. Chatzinotas, and J. Grotz, "Large-scale beam placement and resource allocation design for meo-constellation satcom," in *2023 IEEE International Conference on Communications Workshops (ICC Workshops)*, 2023, pp. 1240–1245.
[3] L. Chen, V. N. Ha, E. Lagunas, L. Wu, S. Chatzinotas, and B. Ottersten, "The next generation of beam hopping satellite systems: Dynamic beam illumination with selective precoding," *IEEE Transactions on Wireless Communications*, vol. 22, no. 4, pp. 2666–2682, 2023.
[4] V. K. Gupta, V. N. Ha, E. Lagunas, H. Al-Hraishawi, L. Chen, and S. Chatzinotas, "Combining time-flexible geo satellite payload with precoding: The cluster hopping approach," *IEEE Transactions on Vehicular Technology*, vol. 72, no. 12, pp. 16 508–16 523, 2023.
[5] E. Lagunas and et al., "Multicast mmse-based precoded satellite systems: User scheduling and equivalent channel impact," in *IEEE VTC2022-Fall*.
[6] T. M. Kebedew, V. N. Ha, E. Lagunas, J. Grotz, and S. Chatzinotas, "Qoe-aware cost-minimizing capacity renting for satellite-as-a-service enabled multiple-beam satcom systems," *IEEE Trans. Commun.*, 2023.
[7] Y. Liu, C. Li, J. Li, and L. Feng, "Robust Energy-Efficient Hybrid Beamforming Design for Massive MIMO LEO Satellite Communication Systems," *IEEE Access*, vol. 10, pp. 63 085–63 099, 2022.
[8] V. N. Ha, T. T. Nguyen, E. Lagunas, J. C. Merlano Duncan, and S. Chatzinotas, "Geo payload power minimization: Joint precoding and beam hopping design," in *IEEE GLOBECOM 2022*, pp. 6445–6450.
[9] V. N. Ha and et al., "Joint linear precoding and dft beamforming design for massive mimo satellite communication," in *IEEE GC Wkshps 2022*.
[10] J. Duncan and et. al., "Hardware precoding demonstration in multibeam uhts communications under realistic payload characteristics," in *ICSSC-2019*, 2019, pp. 1–17.
[11] S. Chatzinotas, G. Zheng, and B. Ottersten, "Energy-efficient mmse beamforming and power allocation in multibeam satellite systems," in *2011 Conference Record of the Forty Fifth Asilomar Conference on Signals, Systems and Computers (ASILOMAR)*, 2011, pp. 1081–1085.
[12] C. Qi, H. Chen, Y. Deng, and A. Nallanathan, "Energy efficient multicast precoding for multiuser multibeam satellite communications," *IEEE Wireless Communications Letters*, vol. 9, no. 4, pp. 567–570, 2020.
[13] T. S. Abdu, S. Kisseleff, E. Lagunas, S. Chatzinotas, and B. Ottersten, "Energy efficient sparse precoding design for satellite communication system," in *VTC2022-Fall*, 2022, pp. 1–6.
[14] V. Joroughi, M. Vazquez, and A. I. Perez-Neira, "Precoding in multigateway multibeam satellite systems," *IEEE Transactions on Wireless Communications*, vol. 15, no. 7, pp. 4944–4956, 2016.
[15] T. Delamotte and A. Knopp, "Smart diversity through mimo satellite q/v-band feeder links," *IEEE Transactions on Aerospace and Electronic Systems*, vol. 56, no. 1, pp. 285–300, 2020.
[16] V. N. Ha, D. H. N. Nguyen, and J.-F. Frigon, "System energy-efficient hybrid beamforming for mmwave multi-user systems," *IEEE Trans. Green Commun. and Netw.*, vol. 4, no. 4, pp. 1010–1023, 2020.
[17] W. Dinkelbach, "On nonlinear fractional programming," *Manage. Sci.*, vol. 13, no. 7, p. 492–498, mar 1967.
[18] V. N. Ha, D. H. N. Nguyen, and J.-F. Frigon, "Subchannel allocation and hybrid precoding in millimeter-wave ofdma systems," *IEEE Transactions on Wireless Communications*, vol. 17, no. 9, pp. 5900–5914, 2018.
[19] ——, "Energy-efficient hybrid precoding for mmwave multi-user systems," in *2018 IEEE ICC*, 2018, pp. 1–6.
[20] V. N. Ha, G. Kaddoum, and G. Poitau, "Joint radio resource management and link adaptation for multicasting 802.11ax-based wlan systems," *IEEE Trans Wireless Commun.*, vol. 20, no. 9, pp. 6122–6138, 2021.
[21] "Hitec-lm-06: 6,8m limited-motion satellite ground antenna system," HITEC Luxembourg S.A., Tech. Rep., June 2020.